

Direct computation of inelastic photon–neutrino processes in the Standard Model

A. Abada, J. Matias and R. Pittau *

Theory Division, CERN, CH-1211 Geneva 23, Switzerland

Abstract

In this paper, we compute the Standard Model polarized amplitudes and cross sections of the processes $\gamma\nu \rightarrow \gamma\gamma\nu$, $\gamma\gamma \rightarrow \gamma\nu\bar{\nu}$ and $\nu\bar{\nu} \rightarrow \gamma\gamma\gamma$, for centre-of-mass energies ω within the range of validity of the Fermi theory. By using a large electron-mass expansion of the exact result, we also derive the first correction term to the effective, low-energy ($\omega < m_e$) formula for $\gamma\nu \rightarrow \gamma\gamma\nu$. Finally, we discuss possible astrophysical implications of our results and provide simple fits to the exact expressions.

Pacs numbers: 13.10.+q, 13.15.+g, 14.70.Bh, 13.88.+e, 95.30.Cq.

CERN-TH/98-241

August 1998

Typeset using REVTeX

*e-mail: abada@mail.cern.ch, matias@mail.cern.ch, pittau@mail.cern.ch.

I. INTRODUCTION

Photon–neutrino processes are potentially of interest in astrophysics and cosmology. Four-leg elastic scattering processes are suppressed by powers of ω/M_W , where ω is the centre-of-mass energy of the collision and M_W the W boson mass [1]. Their cross sections are therefore too small to be of astrophysical interest [2]. On the other hand, five-leg processes involving two neutrinos and three photons, such as

$$\begin{aligned}\gamma\nu &\rightarrow \gamma\gamma\nu \\ \gamma\gamma &\rightarrow \gamma\nu\bar{\nu} \\ \nu\bar{\nu} &\rightarrow \gamma\gamma\gamma,\end{aligned}\tag{1}$$

are not negligible. In fact, the extra α in the cross section is compensated by an interchange of the ω/M_W suppression by an ω/m_e enhancement [3].

In ref. [4], Dicus and Repko derived an effective Lagrangian for the above five-leg photon–neutrino interactions, by substituting one photon with a neutrino current in the Euler–Heisenberg Lagrangian that describes the photon–photon scattering [5]. Some of the formulae reported in ref. [4] were in disagreement with the results derived earlier by Van Hieu and Shabalin [6]. To settle this question, in a recent work [3] we computed the first and the second process in eq. (1), in the framework of the effective theory, confirming the results reported in ref. [4]. We also justified the derivation of the five-leg effective vertex starting from the Euler–Heisenberg Lagrangian.

The effective approach gives reliable results for energies below the threshold for e^+e^- pair production, while its extrapolation to energies above 1 MeV, interesting to study, for example supernova dynamics, is suspect. Therefore, an exact calculation of the processes in eq. (1) is important in order to definitively assess their role in astrophysics and the range of validity of the effective theory. Such a calculation, assuming massless neutrinos, is the main ingredient of this paper. The range of energy in which the above reactions are relevant is well below the W mass, so that we treated the neutrino–electron coupling as a four-Fermi interaction.

Very recently, parallel work in the same direction has been carried out by Dicus, Kao and Repko [7], so that we have a chance to compare our numerical results, finding complete agreement between the two independent calculations.

An additional problem is searching for simple approximations to the exact result. We tried the following two approaches:

- we expanded the exact amplitude in powers of ω/m_e , to derive the first correction term to the effective theory;

- we fitted the curves obtained with the complete calculation.

It turned out that, as expected in ref. [7], an expansion in inverse powers of the electron mass, is not sufficient to extend the range of validity of the effective theory beyond $\omega = m_e$. One is therefore forced to use the complete calculation or fits to it.

The outline of the paper is as follows. In section II, we give the essential steps of the calculation, collecting our final formulae in an appendix. Numerical results are presented in section III, together with the large m_e expansion and the fits. Finally, in section IV, we consider some of the possible astrophysical and cosmological implications of our results.

II. COMPUTATION OF THE AMPLITUDE

The leading Standard Model (SM) diagrams contributing to the processes in eq. (1) are given in fig. 1, where permutations of the photon legs are understood. Momenta and polarization vectors are denoted by the sets $\{i\}$, $\{j\}$ and $\{k\}$ ($i, j, k = 1, 2, 3$), with $\{1\} \equiv \{p_1, \epsilon^\alpha(p_1, \lambda)\}$, $\{2\} \equiv \{p_2, \epsilon^\beta(p_2, \rho)\}$ and $\{3\} \equiv \{p_3, \epsilon^\gamma(p_3, \sigma)\}$, where $\lambda, \rho, \sigma = \pm$. All momenta are incoming and q , flowing in the direction of the fermionic arrow, is the virtual integration momentum.

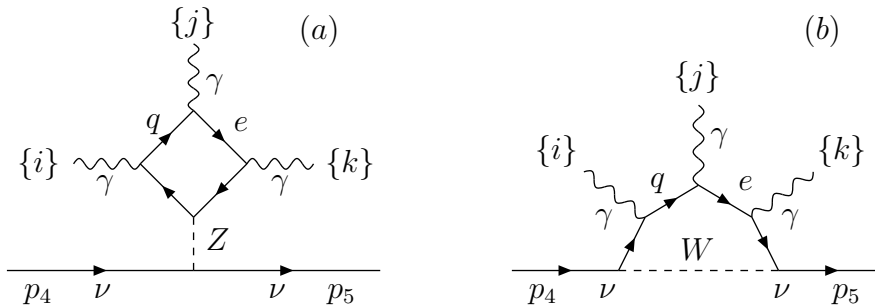


FIG. 1. SM leading diagrams contributing to five-leg photon–neutrino processes.

At low energies, far from the scale of confinement, the leading contribution is given by diagrams involving only electrons in the fermionic loop. It is precisely the appearance of m_e as a scale, instead of M_W (which is the scale governing the four-leg photon–neutrino reactions), that makes such five-leg processes relevant already at energies of the order of a few MeV.

By denoting with A_{ijk} and B_{ijk} the contributions coming from the diagrams (a) and (b) in fig. 1, the total amplitude M reads

$$\begin{aligned}
 M(\lambda, \rho, \sigma) = & [(A_{123} + A_{321}) + (A_{132} + A_{231}) + (A_{213} + A_{312})] \\
 & + [(B_{123} + B_{321}) + (B_{132} + B_{231}) + (B_{213} + B_{312})] ,
 \end{aligned}
 \tag{2}$$

where, for example

$$\begin{aligned}
A_{123} &= - \sum_{\tau=\pm} v_e^\tau \Gamma_\mu \int d^n q \operatorname{Tr} \left[\gamma^\mu w^\tau \frac{1}{Q_{(23)}^-} \not{\epsilon}(p_3, \sigma) \frac{1}{Q_2^-} \not{\epsilon}(p_2, \rho) \frac{1}{Q_0^-} \not{\epsilon}(p_1, \lambda) \frac{1}{Q_{-1}^-} \right] \\
A_{321} &= - \sum_{\tau=\pm} v_e^\tau \Gamma_\mu \int d^n q \operatorname{Tr} \left[\gamma^\mu w^\tau \frac{1}{Q_1^-} \not{\epsilon}(p_1, \lambda) \frac{1}{Q_0^-} \not{\epsilon}(p_2, \rho) \frac{1}{Q_{-2}^-} \not{\epsilon}(p_3, \sigma) \frac{1}{Q_{-(23)}^-} \right]. \quad (3)
\end{aligned}$$

In the previous equations and throughout the calculation, we used the notations

$$\begin{aligned}
Q_{\pm i}^\mp &= Q_{\pm i} \mp m_e, & Q_{\pm(ij)}^\mp &= Q_{\pm(ij)} \mp m_e, \\
Q_{\pm i} &= Q_0 \pm p_i, & Q_{\pm(ij)} &= Q_0 \pm p_i \pm p_j, & Q_0 &= q, \\
D_{\pm i} &= Q_{\pm i}^+ \cdot Q_{\pm i}^-, & D_{\pm(ij)} &= Q_{\pm(ij)}^+ \cdot Q_{\pm(ij)}^-. \quad (4)
\end{aligned}$$

Furthermore, $w^\pm = (1 \pm \gamma_5)/2$, and a dimensional regularization is used to compute each separately divergent diagram. Finally, the current Γ_μ reads

$$\Gamma_\mu = (g s_W)^3 \left(\frac{g}{2c_W} \right)^2 \left(\frac{1}{\Delta_Z} \right) \frac{1}{(2\pi)^4} \bar{v}_+(5) \gamma_\mu u_-(4), \quad (5)$$

and

$$\Delta_Z = (p_4 + p_5)^2 - M_Z^2, \quad v_e^\pm = v_e \pm a_e, \quad v_e = -\frac{1}{2} + 2s_W^2, \quad a_e = \frac{1}{2}, \quad (6)$$

where s_W and c_W are the sine and the cosine of the Weinberg angle, respectively. The reason why the terms in eq. (2) are collected in pairs is because, when adding the two terms in each pair, and using the reversing invariance of the γ -matrix traces, the γ_5 contribution cancels [3]. For example

$$A_{123} + A_{321} = -2v_e \Gamma_\mu \int d^n q \operatorname{Tr} \left[\gamma^\mu \frac{1}{Q_{(23)}^-} \not{\epsilon}(p_3, \sigma) \frac{1}{Q_2^-} \not{\epsilon}(p_2, \rho) \frac{1}{Q_0^-} \not{\epsilon}(p_1, \lambda) \frac{1}{Q_{-1}^-} \right]. \quad (7)$$

Exactly the same work can be applied to each pair of diagrams of type B . For instance, we get

$$B_{123} + B_{321} = -2 \Delta_Z c_W^2 \Gamma_\mu \int d^n q \operatorname{Tr} \left[\gamma^\mu \frac{1}{Q_{(23)}^-} \not{\epsilon}(p_3, \sigma) \frac{1}{Q_2^-} \not{\epsilon}(p_2, \rho) \frac{1}{Q_0^-} \not{\epsilon}(p_1, \lambda) \frac{1}{Q_{-1}^-} \right] \frac{1}{\Delta_W(q)}, \quad (8)$$

where $\Delta_W(q) \equiv (q + p_2 + p_3 + p_5)^2 - M_W^2$. Since we are interested in the large- M_W (or equivalently low-energy) limit, we are allowed to substitute [3]

$$\Delta_Z \sim -M_Z^2 \quad \text{and} \quad \Delta_W \sim -M_W^2, \quad (9)$$

so that the sum of the diagrams in eqs. (7) and (8) gives

$$A_{123} + A_{321} + B_{123} + B_{321} = -2(v_e + 1)\Gamma_\mu I_1^\mu(p_1, p_2, p_3, \lambda, \rho, \sigma) \quad \text{with}$$

$$I_1^\mu(p_1, p_2, p_3, \lambda, \rho, \sigma) = \int d^n q \text{Tr} \left[\gamma^\mu \frac{1}{Q_{(23)}^-} \not{\epsilon}(p_3, \sigma) \frac{1}{Q_2^-} \not{\epsilon}(p_2, \rho) \frac{1}{Q_0^-} \not{\epsilon}(p_1, \lambda) \frac{1}{Q_{-1}^-} \right], \quad (10)$$

where the replacement $\Delta_Z \sim -M_Z^2$ has to be performed also in the current Γ_μ .

Therefore, the total amplitude reads

$$M(\lambda, \rho, \sigma) = -2(1 + v_e) \Gamma_\mu [I_1^\mu(p_1, p_2, p_3, \lambda, \rho, \sigma) + I_2^\mu(p_1, p_2, p_3, \lambda, \rho, \sigma) + I_3^\mu(p_1, p_2, p_3, \lambda, \rho, \sigma)], \quad (11)$$

where I_2^μ and I_3^μ come from the remaining pairs of terms in eq. (2) and can be obtained from I_1^μ as follows

$$I_2^\mu : \quad p_2 \leftrightarrow p_3, \quad \epsilon(p_2, \rho) \leftrightarrow \epsilon(p_3, \sigma)$$

$$I_3^\mu : \quad p_2 \leftrightarrow p_1, \quad \epsilon(p_2, \rho) \leftrightarrow \epsilon(p_1, \lambda). \quad (12)$$

The reduction of $M(\lambda, \rho, \sigma)$ to scalar one-loop integrals can then be performed with the help of the technique described in ref. [8]. The general philosophy of such a method is using the γ algebra in the traces to reconstruct the denominators appearing in the loop integrals, rather than making a more standard tensorial decomposition [9]. The algorithm can be iterated in such a way that only scalar and rank-one functions appear at the end of the reduction, at worst together with higher-rank two-point tensors.

In this paper we content ourselves with giving the first step of this reduction, namely all results expressed only in terms of

- scalar functions with 3 and 4 denominators,
- rank-1 integrals with 3 and 4 denominators,
- rank-2 integrals with 3 denominators,
- rank-3 functions with 3 denominators.

This already provides an important simplification with respect to the standard decomposition, in that the computation of tensors such as

$$T^{\mu\nu; \mu\nu\rho; \mu\nu\rho\sigma} = \int d^n q \frac{q^\mu q^\nu; q^\mu q^\nu q^\rho; q^\mu q^\nu q^\rho q^\sigma}{D_0 D_{-1} D_2 D_{(23)}} \quad (13)$$

is completely avoided.

The key ingredient in the case at hand is a suitable choice of the polarization vectors [10]

$$\begin{aligned}
\epsilon(p_1, \lambda) &= N [\not{p}_2 \not{p}_3 \not{p}_1 w_\lambda + w_\lambda \not{p}_1 \not{p}_3 \not{p}_2] \\
\epsilon(p_2, \rho) &= N [\not{p}_1 \not{p}_3 \not{p}_2 w_\rho + w_\rho \not{p}_2 \not{p}_3 \not{p}_1] \\
\epsilon(p_3, \sigma) &= N [\not{p}_1 \not{p}_2 \not{p}_3 w_\sigma + w_\sigma \not{p}_3 \not{p}_2 \not{p}_1] ,
\end{aligned} \tag{14}$$

where

$$N = \left(\frac{1}{4(p_1 \cdot p_2)(p_1 \cdot p_3)(p_2 \cdot p_3)} \right)^{\frac{1}{2}} \quad \text{and} \quad w_\pm = \frac{1}{2}(1 \pm \gamma_5). \tag{15}$$

Inserting eq. (14) in the expression for I_2^μ and using the identity

$$\not{p}_2 \not{p}_3 \not{p}_1 w^\lambda + w^\lambda \not{p}_1 \not{p}_3 \not{p}_2 = -(\not{p}_3 \not{p}_2 \not{p}_1 w^\lambda + w^\lambda \not{p}_1 \not{p}_2 \not{p}_3) + 2(p_2 \cdot p_3) [Q_0^- - Q_{-1}^-], \tag{16}$$

gives

$$\begin{aligned}
I_2^\mu(p_1, p_2, p_3, \lambda, \rho, \sigma) &= -I_1^\mu(p_1, p_3, p_2, \lambda, \sigma, \rho) + J_2^\mu(p_1, p_2, p_3, \rho, \sigma) \quad \text{with} \\
J_2^\mu(p_1, p_2, p_3, \rho, \sigma) &= 2(p_2 \cdot p_3) N^3 \left\{ \int d^n q \text{Tr} \left[\gamma^\mu \frac{1}{Q_{(23)}^-} (\not{p}_1 \not{p}_3 \not{p}_2 w^\rho + w^\rho \not{p}_2 \not{p}_3 \not{p}_1) \right. \right. \\
&\quad \left. \left. \times \frac{1}{Q_3^-} (\not{p}_1 \not{p}_2 \not{p}_3 w^\sigma + w^\sigma \not{p}_3 \not{p}_2 \not{p}_1) \left(\frac{1}{Q_{-1}^-} - \frac{1}{Q_0^-} \right) \right] \right\}.
\end{aligned} \tag{17}$$

With similar arguments we also get

$$\begin{aligned}
I_3^\mu(p_1, p_2, p_3, \lambda, \rho, \sigma) &= -I_1^\mu(p_2, p_1, p_3, \rho, \lambda, \sigma) + J_3^\mu(p_1, p_2, p_3, \lambda, \rho) \quad \text{with} \\
J_3^\mu(p_1, p_2, p_3, \lambda, \rho) &= 2(p_1 \cdot p_2) N^3 \left\{ \int d^n q \text{Tr} \left[\gamma^\mu \left(\frac{1}{Q_1^-} - \frac{1}{Q_{(13)}^-} \right) (\not{p}_2 \not{p}_3 \not{p}_1 w^\lambda + w^\lambda \not{p}_1 \not{p}_3 \not{p}_2) \right. \right. \\
&\quad \left. \left. \times \frac{1}{Q_0^-} (\not{p}_1 \not{p}_3 \not{p}_2 w^\rho + w^\rho \not{p}_2 \not{p}_3 \not{p}_1) \frac{1}{Q_{-2}^-} \right] \right\}.
\end{aligned} \tag{18}$$

Therefore, since J_2^μ and J_3^μ are directly expressed in terms of differences of three-point functions, I_1^μ given in eq. (10) is the only master integral we need to decompose in terms of simpler tensorial structures. By inserting eq. (14) into eq. (10) for each combination of photon helicities, we obtain four different expressions. For example, when $\rho = \sigma = -\lambda$:

$$I_1^\mu(p_1, p_2, p_3, \lambda, -\lambda, -\lambda) = N^3 \int d^n q \frac{1}{D_0 D_{-1} D_2 D_{(23)}} A^\mu(\lambda, -\lambda, -\lambda), \tag{19}$$

with

$$\begin{aligned}
A^\mu(\lambda, -\lambda, -\lambda) &= m_e^2 ([\mu Q_{(23)} 123231 Q_0 231]_\lambda + [\mu Q_{-1} 132 Q_0 132321]_\lambda \\
&\quad + [\mu 231 Q_0 231 Q_2 321]_\lambda + [\mu 321 Q_2 231 Q_0 231]_\lambda) \\
&\quad + [\mu Q_{-1} 132 Q_0 132 Q_2 123 Q_{(23)}]_\lambda + [\mu Q_{(23)} 123 Q_2 132 Q_0 132 Q_{-1}]_\lambda, \quad (20)
\end{aligned}$$

and where we used the notation $[\mu i j k \dots]_\lambda = \text{Tr}[\gamma^\mu \not{p}_i \not{p}_j \not{p}_k \dots w^\lambda]$.

To illustrate how the reduction works, take for example the last term in eq. (20). Since $p_3 \cdot p_3 = 0$, we may rewrite

$$[\mu Q_{(23)} 123 Q_2 132 Q_0 132 Q_{-1}]_\lambda = -[\mu Q_{(23)} 1231 Q_2 32 Q_0 132 Q_{-1}]_\lambda, \quad (21)$$

and, from the identity

$$Q_2 \not{p}_3 \not{p}_2 Q_0 = (D_{(23)} - D_2) \not{p}_2 Q_0 + (D_0 - D_2) \not{p}_3 Q_0 + (D_0 + m_e^2) \not{p}_3 \not{p}_2, \quad (22)$$

the first step of the denominator reconstruction immediately follows. As a second example, consider a term such as $[\mu \dots 1 Q_0 1 \dots]_\lambda$. Since $\not{p}_1 \not{p}_1 = \not{p}_1 (D_0 - D_{-1})$, we immediately get

$$[\mu \dots 1 Q_0 1 \dots]_\lambda = (D_0 - D_{-1}) [\mu \dots 1 \dots]_\lambda, \quad \text{etc.} \quad (23)$$

The final result of such a procedure is given in the appendix. An important remark is in order here. To obtain compact expressions, we made a large use of the Kahane–Chisholm manipulations over γ matrices [11]. Such identities are strictly four-dimensional, while we are, at the same time, using dimensional regularization. Our solution is splitting, *before any trace manipulation*, the n -dimensional integration momentum appearing in the traces as [8]

$$q \rightarrow q + \tilde{q}, \quad (24)$$

where q and \tilde{q} are the four-dimensional and ϵ -dimensional components ($\epsilon = n - 4$), respectively, so that $q \cdot \tilde{q} = 0$. The γ algebra can then be safely performed in four dimensions, at the price of having additional terms. In fact, the splitting in eq. (24) is equivalent to redefining $m_e^2 \rightarrow m_e^2 - \tilde{q}^2$ from the beginning. The net effect is then the appearance of extra integrals containing powers of \tilde{q}^2 in the numerator, whenever m_e^2 is present in the formulae reported in the appendix. The computation of such integrals in the limit $\epsilon \rightarrow 0$ is straightforward [8]. For example

$$\begin{aligned}
\int d^n q \frac{\tilde{q}^4}{D_0 D_{-1} D_2 D_{(23)}} &= -i \frac{\pi^2}{6} + \mathcal{O}(\epsilon), \\
\int d^n q \frac{q_\mu \tilde{q}^2}{D_0 D_{-1} D_2} &= i \frac{\pi^2}{6} (p_2 - p_1)_\mu + \mathcal{O}(\epsilon). \quad (25)
\end{aligned}$$

A standard Passarino–Veltman decomposition [9] of the simple remaining tensorial structures in terms of scalar loop functions, concludes our calculation. We implemented the outgoing formulae in a Fortran code, performing the phase-space integration by Monte Carlo. Numerical results are reported in the next section.

Our formulae remain valid also when including all neutrino species. In this case, only the first diagram in fig. 1a contributes, at leading order in ω/m_e , because the second one is suppressed by powers of $\omega/m_{\mu,\tau}$. Therefore, the inclusion of all neutrinos can be achieved by simply replacing $(1 + v_e)$ with $(1 + 3 v_e)$ in eq. (11). However, we only considered ν_e in our numerical results.

III. RESULTS

In this section, we give numerical results for the three reactions in eq. (1) and present simple approximations to the full computation. Our main motivations are to assess the range of validity of the effective theory, and go beyond it.

The total cross sections computed using the effective Euler–Heisenberg Lagrangian are [3,4]

$$\begin{aligned}\sigma^{eff}(\gamma\nu \rightarrow \gamma\gamma\nu) &= \frac{262}{127575} k^2 \left(\frac{\omega}{m_e}\right)^{10} \\ \sigma^{eff}(\gamma\gamma \rightarrow \gamma\nu\bar{\nu}) &= \frac{2144}{637875} k^2 \left(\frac{\omega}{m_e}\right)^{10} \\ \sigma^{eff}(\nu\bar{\nu} \rightarrow \gamma\gamma\gamma) &= \frac{136}{91125} k^2 \left(\frac{\omega}{m_e}\right)^{10},\end{aligned}\tag{26}$$

with $k = G_F m_e (1 + v_e) \alpha^{3/2}/\pi^2$. Effective and exact computations are compared in figs. 2, 3 and 4, for the three cases. Furthermore, table I shows the ratio between exact cross section and σ^{eff} for several values of ω/m_e .

From the above figures and numbers it is clear that, for all three processes, the effective theory is valid only when, roughly, $\omega/m_e \leq 2$, as expected. At larger ω , the exact computation predicts a softer energy dependence with respect to the $(\omega/m_e)^{10}$ behaviour given by the effective Lagrangian.

All above results are in full agreement with those reported in ref. [7]. Notice also that exact and effective predictions approach each other in the limit of vanishing ω , as it should be. This provides us with an additional, strong numerical check on the correctness of our computation.

Since the exact formulae are quite involved, we found it convenient to look for an approximation above the point $\omega/m_e = 2$. With this aim, we performed a large- m_e expansion of the integrals in eqs. (10) and (12), to determine the $\mathcal{O}(1/m_e^6)$ correction to the effective amplitude for $\gamma\nu \rightarrow \gamma\gamma\nu$. By iteratively applying the equation

$$\frac{1}{((q+k)^2 - m_e^2)} = \frac{1}{q^2 - m_e^2} - \frac{k^2 + 2q \cdot k}{(q^2 - m_e^2)((q+k)^2 - m_e^2)},\tag{27}$$

and systematically discarding terms smaller than $\mathcal{O}(1/m_e^6)$, one is left with only contributions of the kind

$$m_e^r p^s \int d^n q \frac{q^t}{(q^2 - m_e^2)^l}, \quad (28)$$

in which the external momentum dependence is factorized out from the integrals. In the above formula, p^s stands for any product of s external momenta, and t, l, r, s are constrained by $4 + r + t - 2l + s = 0$. Thus, when $r + s = 0$ the integral in eq. (28) is divergent, when $r + s = 2$ it is finite and proportional to $1/m_e^2$, and so on.

By summing all relevant contributions, we found

$$\sigma(\gamma\nu \rightarrow \gamma\gamma\nu) = \frac{m_e^2 G_F^2 (1 + v_e)^2 \alpha^3}{127575 \pi^4} \left(262 \left(\frac{\omega}{m_e} \right)^{10} - \frac{3163}{20} \left(\frac{\omega}{m_e} \right)^{12} \right). \quad (29)$$

The first term in the r.h.s. of eq. (29) coincides with the result given in eq. (26), so this is an extra check of our computation. The second term has the right sign but, as expected in ref. [7], it does not give numerical predictions that are useful to extend the effective theory beyond $\omega = m_e$. The only option is then to fit the curves in figs. 2, 3 and 4. The results of the fits are

$$\begin{aligned} \sigma(\gamma\nu \rightarrow \gamma\gamma\nu) &= \sigma^{eff}(\gamma\nu \rightarrow \gamma\gamma\nu) \times r^{-2.76046} \\ &\times \exp[2.13317 - 2.12629 \log^2(r) + 0.406718 \log^3(r) - 0.029852 \log^4(r)], \\ \sigma(\gamma\gamma \rightarrow \gamma\nu\bar{\nu}) &= \sigma^{eff}(\gamma\gamma \rightarrow \gamma\nu\bar{\nu}) \times r^{-7.85491} \\ &\times \exp[4.42122 + 0.343516 \log^2(r) - 0.114058 \log^3(r) + 0.0103219 \log^4(r)], \\ \sigma(\nu\bar{\nu} \rightarrow \gamma\gamma\gamma) &= \sigma^{eff}(\nu\bar{\nu} \rightarrow \gamma\gamma\gamma) \times r^{-6.57374} \\ &\times \exp[5.27548 - 0.689808 \log^2(r) + 0.15014 \log^3(r) - 0.0123385 \log^4(r)], \end{aligned} \quad (30)$$

where the effective cross sections σ^{eff} are given in eq. (26), and $r = \omega/m_e$. All the above fits are valid in the energy range $1.7 < r < 100$.

IV. DISCUSSION AND CONCLUDING REMARKS

The processes $\nu\gamma \rightarrow \nu\gamma\gamma$, $\nu\bar{\nu} \rightarrow \gamma\gamma\gamma$ and $\gamma\gamma \rightarrow \gamma\nu\bar{\nu}$ are of potential interest in stellar evolution and cosmology. The first two reactions can affect the mean free path of neutrinos inside the supernova core, while the last one is a possible cooling mechanism for hot objects [12]. The relevance of such processes depends on the size of the cross sections when varying the centre-of-mass energy ω , and may be definitively assessed only through complete and detailed Monte Carlo simulations. Nevertheless, some simple considerations can be made, also in connection with speculations that recently appeared in the literature.

Basing their results on the assumption

$$\sigma(\gamma\nu \rightarrow \gamma\gamma\nu) = \sigma_0 \left(\frac{\omega}{1 \text{ MeV}} \right)^\gamma, \quad \sigma_0 = 10^{-52} \text{ cm}^2, \quad (31)$$

and on the data collected from supernova 1987A, the authors of ref. [12] fitted the exponent γ in eq. (31) to be less than 8.4, for ω of the order of a few MeV. The physical requirement behind this is that neutrinos of a few MeV should immediately leave the supernova, so that their mean free path is constrained to be larger than 10^{11} cm.

The effective theory predicts $\gamma = 10$, while, using the exact calculation, a softer energy dependence is observed in the region of interest (see fig. 2). A fit to the exact curve gives $\gamma \sim 3$ for $1 \text{ MeV} < \omega < 10 \text{ MeV}$, thus confirming the expectations of ref. [12].

A second interesting quantity is the range of parameters for which the neutrino mean free path for such reactions is inside the supernova core, therefore affecting its dynamics. Always in ref. [12] it was found, with the help of Monte Carlo simulations, that for several choices of temperature and chemical potential, and assuming the validity of the effective theory ($\gamma = 10$), this happens when $\omega \geq 5 \text{ MeV}$. Since the exact results are now available, it would be of extreme interest to see how the above prediction is affected. More in general, we think that the reactions in eq. (1) should be included in supernova codes.

In ref. [4], it was speculated that these processes could also have some relevance in cosmology. Consider, in fact, the mean number \bar{N} of neutrino collisions, via the first reaction in eq. (1), in an expansion time t equal to the age of the Universe [13]:

$$\bar{N} = \sigma(\gamma\nu \rightarrow \gamma\gamma\nu)n_\nu ct, \quad n_\nu = \text{neutrino number density}. \quad (32)$$

In the above formula, n_ν and t can be rewritten in terms of the photon energy at thermal equilibrium ($\omega \sim kT$), expressed in units of 10^{10} K. By denoting this quantity by T_{10} , we get

$$n_\nu = 1.6 \times 10^{31} T_{10}^3 \text{ cm}^{-3}, \quad t = 2 T_{10}^{-2} \text{ s}. \quad (33)$$

When \bar{N} is large, the neutrinos are in thermal contact with matter and radiation, while, for $\bar{N} \sim 1$ (namely $\sigma \sim 10^{-42} T_{10}^{-1} \text{ cm}^2$), the neutrinos decouple. By using the formula in eq. (26), the resulting decoupling temperature is $T_{10} \sim 9.5$, namely $\omega \sim 8.2 \text{ MeV}$, therefore outside the range of validity of the effective theory. By repeating the same analysis with the exact result, we found instead that \bar{N} becomes of the order of 1 at $\omega \sim 1 \text{ GeV}$. At these energies, other processes enter the game; for instance reactions involving different leptons, quarks and hadrons inside the loop in fig. 1a. Therefore, the reaction $\gamma\nu \rightarrow \gamma\gamma\nu$ is no longer the only relevant process. In conclusion, the five-leg reactions in eq. (1) are unlikely to be important for a study of the neutrino decoupling temperature, contrary to what the effective theory seemed to suggest.

ACKNOWLEDGEMENTS

We thank the authors of ref. [7] for having informed us about their recent computation. We also wish to thank M. B. Gavela, G. F. Giudice and O. Pène for helpful discussions, and G. Passarino for numerical checks on the loop functions. J.M. acknowledges the financial support from a Marie Curie EC Grant (TMR-ERBFMBICT 972147).

Appendix

We list here the result of the decomposition of the master integral in eq. (10), performed with the technique of ref. [8]. The starting point is the formula

$$I_1^\mu(p_1, p_2, p_3, \lambda, \rho, \sigma) = N^3 \int d^n q \frac{1}{D_0 D_{-1} D_2 D_{(23)}} A^\mu(\lambda, \rho, \sigma), \quad (34)$$

with N given in eq. (15).

By defining $(i \cdot j) \equiv p_i \cdot p_j$ and $m \equiv m_e$, the four possible helicity configurations read

- $\lambda = -\rho = -\sigma$:

$$\begin{aligned} A^\mu(\lambda, -\lambda, -\lambda) = & -4(1 \cdot 2)(2 \cdot 3) D_0 \left\{ [\mu Q_0 132 Q_0 13]_\lambda + 2(1 \cdot 3) [\mu Q_{(23)} 132 Q_{-1}]_\lambda \right\} \\ & + (D_{(23)} - D_2) \left\{ 4m^2(1 \cdot 2) [[\mu 231 Q_0 231]_\lambda - 2[\mu 1(Q_0 2 - 2Q_0)]_\lambda (1 \cdot 3)(2 \cdot 3)] \right. \\ & \left. - [\mu Q_{(23)} 1231 Q_0 231 2 Q_{-1}]_\lambda - [\mu Q_0 1321 Q_0 231 Q_0 2]_\lambda \right\} \\ & + (D_0 - D_2) \left\{ 2(1 \cdot 3) m^2 [4(1 \cdot 2)(2 \cdot 3) [\mu 1(3Q_0 - Q_0 3)]_\lambda + [\mu(32 - 23) Q_0 1231]_\lambda] \right. \\ & \left. - 2[\mu Q_{(23)} 123 Q_0 132 Q_{-1}]_\lambda (1 \cdot 3) + [\mu Q_0 1321 Q_0 23 Q_0 13]_\lambda \right\} \\ & - 16m^2(1 \cdot 2)(1 \cdot 3)(2 \cdot 3)(D_0 - D_{-1}) [\mu 32 Q_0]_\lambda \\ & + 8(1 \cdot 2)(1 \cdot 3)(2 \cdot 3)(D_0 + m^2) m^2 \{ [\mu 132]_\lambda - [\mu 123]_\lambda + [\mu 321]_\lambda - [\mu 231]_\lambda \} \\ & + 8m^2(1 \cdot 2)(1 \cdot 3)(2 \cdot 3) \{ -[\mu Q_0 1231]_\lambda + 2(2 \cdot 3) [\mu 1(Q_0 2 - 2Q_0)]_\lambda \\ & - 2(1 \cdot 2) [\mu 231]_\lambda + [\mu 231 2 Q_0]_\lambda - 2(1 \cdot 3) [\mu 32 Q_{-1}]_\lambda \} \\ & - 4m^2(1 \cdot 3)(2 \cdot 3) [\mu 321 Q_0 231]_\lambda. \end{aligned} \quad (35)$$

- $\lambda = \rho = \sigma$:

$$\begin{aligned} A^\mu(\lambda, \lambda, \lambda) = & 8m^2(1 \cdot 2)(1 \cdot 3)(2 \cdot 3)(D_{(23)} - D_2) [\mu 2(Q_0 1 - 1Q_0)]_\lambda \\ & - 4(1 \cdot 3)(2 \cdot 3)(D_0 - D_2) \left\{ [\mu Q_0 1 Q_2 321 Q_{(23)}]_\lambda \right. \\ & \left. + m^2 [[\mu 123 Q_2 1]_\lambda - [\mu 1321 Q_0]_\lambda + 2(1 \cdot 3) [\mu 21 Q_0]_\lambda - 2(1 \cdot 2) [\mu 3 Q_0 1]_\lambda] \right\} \\ & + 4(1 \cdot 3)(2 \cdot 3)(D_0 - D_{-1}) \left\{ [\mu Q_2 321 Q_0 2 Q_{-1}]_\lambda \right. \\ & \left. + m^2 [[\mu 231 2 Q_0]_\lambda + [\mu 2 Q_0 123]_\lambda + 2(2 \cdot 3) ([\mu 21 Q_{(23)}]_\lambda - [\mu 121]_\lambda) - 2(1 \cdot 2) [\mu Q_0 32]_\lambda] \right\} \\ & + 16(1 \cdot 2)(1 \cdot 3)(2 \cdot 3)(D_0 + m^2) m^2 \{ [3(2 \cdot 3) - 2(1 \cdot 2)] [\mu 1]_\lambda \\ & - 2[\mu 123]_\lambda - 2 [(1 \cdot 3) + (1 \cdot 2)] [\mu 2]_\lambda \} \\ & - 8m^2(1 \cdot 2)(1 \cdot 3)(2 \cdot 3) \left\{ [\mu 21 Q_0 32]_\lambda - [\mu 123 Q_0 1]_\lambda + 2(2 \cdot 3) \{ [m^2 - 4(1 \cdot 2)] [\mu 1]_\lambda \right. \\ & \left. + [\mu Q_0 12]_\lambda + [\mu Q_0 13]_\lambda + [\mu 12 Q_0]_\lambda - [\mu 123]_\lambda \} \right\} + 4m^2(1 \cdot 3)(2 \cdot 3) [\mu 21 Q_0 3123]_\lambda. \end{aligned} \quad (36)$$

- $\lambda = \rho = -\sigma$:

$$\begin{aligned}
A^\mu(\lambda, \lambda, -\lambda) = & -16 m^2(1 \cdot 2)(1 \cdot 3)(2 \cdot 3)(D_{(23)} - D_2)[\mu 12Q_0]_\lambda \\
& -4(1 \cdot 3)(2 \cdot 3)(D_0 - D_2) \{ [\mu Q_0 1 Q_2 123 Q_2]_\lambda \\
& + m^2 [[\mu 321 Q_2 1]_\lambda - [\mu 21321]_\lambda - [\mu 31321]_\lambda + 4(1 \cdot 2)[\mu 13Q_0]_\lambda] \} \\
& +4(1 \cdot 3)(2 \cdot 3)(D_0 - D_{-1}) \{ [\mu Q_{(23)} 123 Q_0 2 Q_{-1}]_\lambda \\
& + m^2 [[\mu 23Q_0 12]_\lambda + 2(1 \cdot 2) \{ [\mu 23Q_2]_\lambda - [\mu 321]_\lambda - 4[\mu 23Q_0]_\lambda + 2(2 \cdot 3)[\mu Q_0]_\lambda \}] \} \\
& +16(1 \cdot 2)(1 \cdot 3)(2 \cdot 3)(D_0 + m^2)m^2 \{ [\mu 123]_\lambda - (2 \cdot 3)[\mu 1]_\lambda \} \\
& +8 m^2(1 \cdot 2)(1 \cdot 3)(2 \cdot 3) \{ [\mu 23Q_0 12]_\lambda - [\mu 2312Q_0]_\lambda + [\mu 321Q_0 1]_\lambda - [\mu Q_0 1321]_\lambda \\
& + m^2 [\mu(23 - 32)1]_\lambda + 2(1 \cdot 3)[\mu 32Q_{-1}]_\lambda \\
& + 2(2 \cdot 3) [-[\mu Q_0 12]_\lambda + 2[\mu 12Q_0]_\lambda - 2(1 \cdot 2)[\mu 2]_\lambda] \\
& + 2(1 \cdot 2) [-2[\mu 23Q_0]_\lambda - [\mu 32Q_0]_\lambda + 2(2 \cdot 3)[\mu 1]_\lambda] \} \\
& +4 m^2(1 \cdot 3)(2 \cdot 3) \{ [\mu 3213Q_0 21]_\lambda - 2(2 \cdot 3)[\mu 21Q_0 12]_\lambda \} . \tag{37}
\end{aligned}$$

- $\lambda = -\rho = \sigma$:

$$\begin{aligned}
A^\mu(\lambda, -\lambda, \lambda) = & 4 D_0(1 \cdot 2)(2 \cdot 3) \left\{ 2(1 \cdot 3) \{ [m^2 + 2(1 \cdot 2)] [\mu 231]_\lambda \right. \\
& + 2 [(1 \cdot 2)[\mu 32Q_0]_\lambda + (2 \cdot 3)[\mu Q_0 12]_\lambda + (2 \cdot 3)[\mu Q_0 13]_\lambda] \} + [\mu Q_0 132Q_0 31]_\lambda \} \\
& +4(D_2 - D_{(23)})(1 \cdot 2)(2 \cdot 3) \left\{ 4(1 \cdot 3) [m^2 + (2 \cdot 3)] [\mu 12Q_0]_\lambda - 2(2 \cdot 3)[\mu 12Q_0 31]_\lambda \right. \\
& + 2(1 \cdot 2) \{ 2(2 \cdot 3)[\mu 12Q_0]_\lambda - 2(2 \cdot 3)[\mu 1Q_0 2]_\lambda + [\mu 12Q_0 31]_\lambda + [\mu 2132Q_0]_\lambda \} \\
& + [\mu 1Q_0 2312Q_0]_\lambda - [\mu Q_0 1321Q_0 2]_\lambda + [\mu Q_0 132Q_0 13]_\lambda \} \\
& -8(D_0 - D_2)(1 \cdot 2)(2 \cdot 3) \left\{ 2(1 \cdot 3) \{ [m^2 + (2 \cdot 3)] [\mu 13Q_0]_\lambda - (1 \cdot 2)[\mu 23Q_0]_\lambda \right. \\
& + (1 \cdot 2) [4(2 \cdot 3)[\mu 13Q_0]_\lambda + [\mu 13Q_0 31]_\lambda] - (2 \cdot 3) [[\mu 13Q_0 21]_\lambda + [\mu 13Q_0 31]_\lambda] \} \\
& -2(D_0 - D_{-1})(2 \cdot 3) \left\{ 4(1 \cdot 2)^2 [\mu 3Q_0 231]_\lambda + m^2 [\mu 213Q_0 231]_\lambda - m^2 [\mu 2312Q_0 13]_\lambda \right. \\
& + 2(2 \cdot 3)[\mu Q_0 13Q_0 213]_\lambda - 2(1 \cdot 2) \{ 4(2 \cdot 3)^2 [\mu 12Q_0]_\lambda + 4 m^2(1 \cdot 3)[\mu 32Q_0]_\lambda \\
& + 2(2 \cdot 3) [2(1 \cdot 3)[\mu 32Q_0]_\lambda - [\mu 2312Q_0]_\lambda - [\mu 321Q_0 2]_\lambda + [\mu 3Q_0 231]_\lambda - [\mu Q_0 13Q_0 2]_\lambda] \\
& + [\mu 3Q_0 2312Q_0]_\lambda + [\mu Q_0 31Q_0 231]_\lambda \} + [\mu 21321Q_0 231]_\lambda + [\mu 231Q_0 2312Q_0]_\lambda \\
& \left. - [\mu Q_0 13Q_0 2312Q_0]_\lambda - [\mu Q_0 31Q_0 2132Q_0]_\lambda \} \right.
\end{aligned}$$

$$\begin{aligned}
& -8(D_0 + m^2)(1 \cdot 2)(2 \cdot 3) \{4(1 \cdot 2)(2 \cdot 3)\{(1 \cdot 3)([\mu 1]_\lambda - [\mu 2]_\lambda) + [\mu 132]_\lambda\} \\
& + (1 \cdot 3) \left[-4(2 \cdot 3)^2[\mu 1]_\lambda + 2(2 \cdot 3)[\mu 132]_\lambda + m^2(2[\mu 132]_\lambda - [\mu 231]_\lambda) \right] \} \\
& + 4(2 \cdot 3) \left\{ m^2(1 \cdot 3)[\mu 231 Q_0 213]_\lambda + 2(1 \cdot 2)^2 \{4(2 \cdot 3)^2([\mu 12 Q_0]_\lambda - [\mu 1 Q_0 2]_\lambda) \right. \\
& + 2m^2(1 \cdot 3)([\mu 231]_\lambda + [\mu 32 Q_0]_\lambda) + 2(2 \cdot 3)([\mu 12 Q_0 31]_\lambda + [\mu 2132 Q_0]_\lambda) + [\mu 231 Q_0 231]_\lambda \} \\
& + (1 \cdot 2) \{-4(2 \cdot 3)^2[\mu 12 Q_0 31]_\lambda - 2(1 \cdot 3)[\mu 12 Q_0]_\lambda \} \\
& + 2(1 \cdot 3) \left[2m^2(2 \cdot 3)(2[\mu 12 Q_0]_\lambda + [\mu Q_0 12]_\lambda + [\mu Q_0 13]_\lambda) \right. \\
& \left. + m^2(m^2[\mu 231]_\lambda - [\mu 1 Q_0 231]_\lambda + [\mu 231 Q_0 2]_\lambda) \right] + m^2([\mu 231 2 Q_0 13]_\lambda + [\mu 231 Q_0 231]_\lambda) \} \}.
\end{aligned} \tag{38}$$

The expressions for I_2^μ and I_3^μ are given in terms of I_1^μ in eqs. (17) and (18).

Another advantage of the above reduction technique is the possibility of checking the calculation without explicitly computing the loop integrals. For example, with any arbitrary choice of p_1, p_2, p_3, q and $m_e \equiv m$, the expressions in eqs. (20) and (35) should coincide numerically.

REFERENCES

- [1] C. N. Yang, Phys. Rev. **77** (1950) 242;
M. Gell-Mann, Phys. Rev. Lett. **6** (1961) 70.
- [2] D. A. Dicus and W. W. Repko, Phys. Rev. **D48** (1993) 5106;
A. Abbasabadi, A. Devoto, D. A. Dicus and W. W. Repko, “*High energy photon-neutrino interactions*”, hep-ph/9808211.
- [3] A. Abada, J. Matias and R. Pittau, “*Inelastic photon–neutrino interactions using an effective Lagrangian*”, hep-ph/9806383.
- [4] D. A. Dicus and W. W. Repko, Phys. Rev. Lett. **79** (1997) 569.
- [5] H. Euler, Ann. Phys. **26**, 398 (1936); W. Heisenberg and H. Euler, Z. Phys. **98**, 714 (1936).
- [6] N. Van Hieu and E. P. Shabalin, Sov. Phys. JETP **17** (1963) 681.
- [7] D. A. Dicus, C. Kao and W. W. Repko, “ $\gamma\nu \rightarrow \gamma\gamma\nu$ and crossed processes at energies below m_W ”, hep-ph/9806499.
- [8] R. Pittau, Comput. Phys. Commun. 104 (1997) 23 and 111 (1998) 48.
- [9] G. Passarino and M. Veltman, Nucl. Phys. **B160** (1979) 151.
- [10] F. A. Berends et al., Phys. Lett. **B103** (1981) 124;
P. De Causmaecker et al., Nucl. Phys. **B206** (1982) 53;
R. Kleiss and W. J. Stirling, Nucl. Phys. **B262** (1985) 235;
J. F. Gunion and Z. Kunszt, Phys. Lett. **B161** (1985) 333;
Z. Xu, D. -H. Zhang and L. Chang, Nucl. Phys. **B291** (1987) 392.
- [11] J. Kahane, J. Math. Phys. **9** (1968) 1732;
J. S. R. Chisholm, Comput. Phys. Commun. **4** (1972) 205;
E. R. Caianiello and S. Fubini, Nuovo Cimento **9** (1952) 1218.
- [12] M. Harris, J. Wang and V. L. Teplitz, “*Astrophysical effects of $\nu\gamma \rightarrow \nu\gamma\gamma$ and its crossed processes*”, astro-ph/9707113.
- [13] P. J. E. Peebles, “*Principles of Physical Cosmology*” (Princeton University Press, Princeton, New Jersey, 1993).

TABLES

ω/m_e	$\gamma\nu \rightarrow \gamma\gamma\nu$	$\gamma\gamma \rightarrow \gamma\nu\bar{\nu}$	$\nu\bar{\nu} \rightarrow \gamma\gamma\gamma$
0.3	0.969(8)	1.09(1)	1.20(1)
0.4	0.923(6)	1.17(1)	1.37(1)
0.5	0.888(6)	1.28(1)	1.68(1)
0.6	0.852(4)	1.47(1)	2.20(1)
0.7	0.826(5)	1.80(1)	3.17(1)
0.8	0.811(5)	2.41(1)	5.31(2)
0.9	0.819(6)	3.95(2)	11.88(3)
1.0	0.880(7)	23.1(1)	176.3(3)
1.1	1.19(1)	18.2(1)	94.7(2)
1.3	1.71(2)	8.31(5)	31.6(1)
1.5	1.44(1)	3.37(2)	11.9(1)
1.7	0.996(8)	1.40(1)	4.96(3)
1.9	0.635(4)	0.622(3)	2.23(1)
2.0	0.503(3)	0.424(2)	1.54(1)

TABLE I. Ratio between exact and effective results for the three cross sections. The error on the last digit comes from the phase-space Monte Carlo integration.

FIGURES

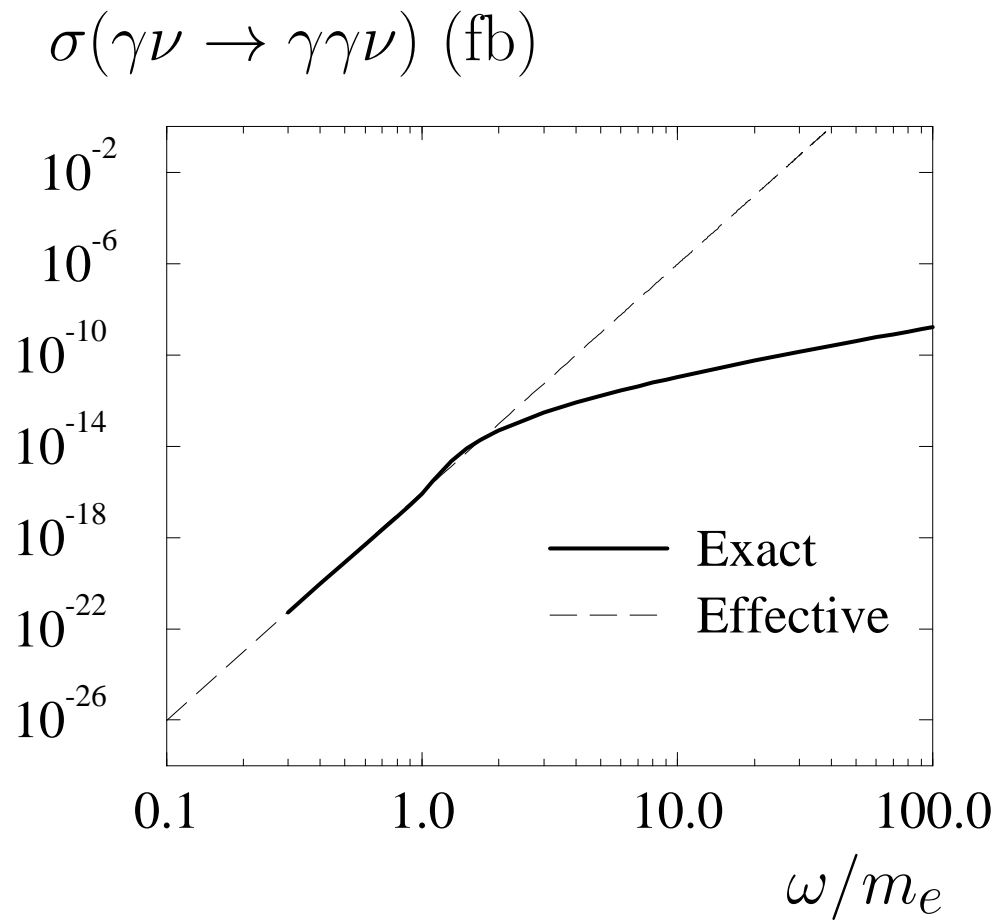


FIG. 2. $\gamma\nu \rightarrow \gamma\gamma\nu$ cross section in fb as a function of ω/m_e .

$$\sigma(\gamma\gamma \rightarrow \gamma\nu\bar{\nu}) \text{ (fb)}$$

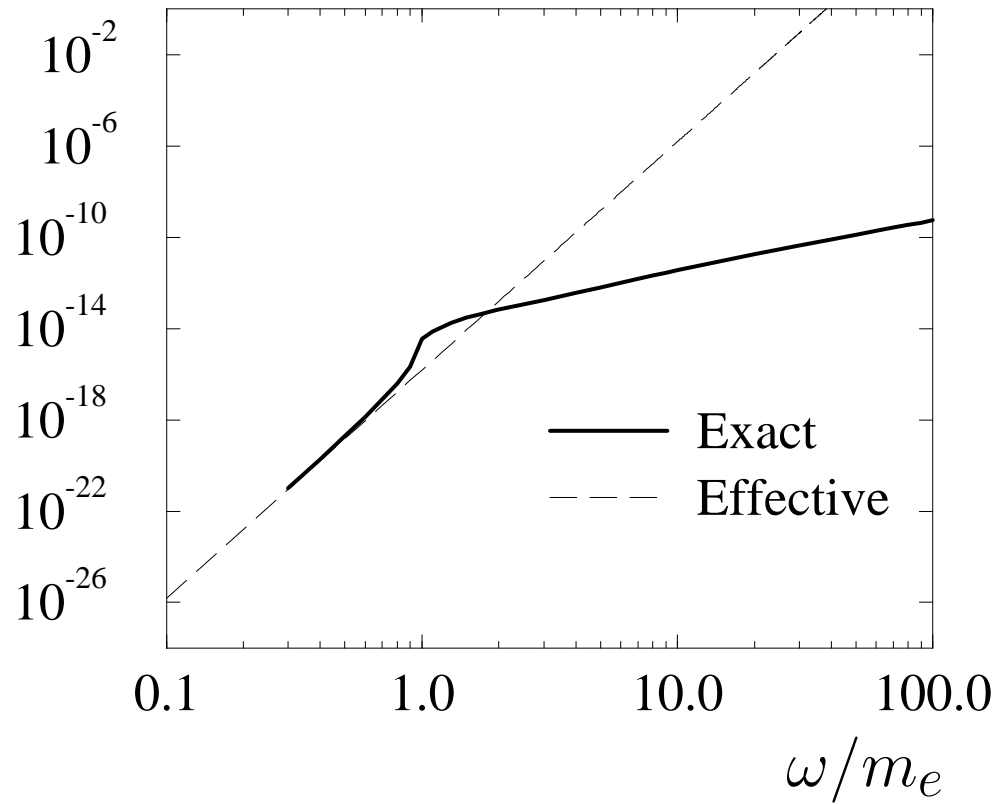


FIG. 3. $\gamma\gamma \rightarrow \gamma\nu\bar{\nu}$ cross section in fb as a function of ω/m_e .

$$\sigma(\nu\bar{\nu} \rightarrow \gamma\gamma\gamma) \text{ (fb)}$$

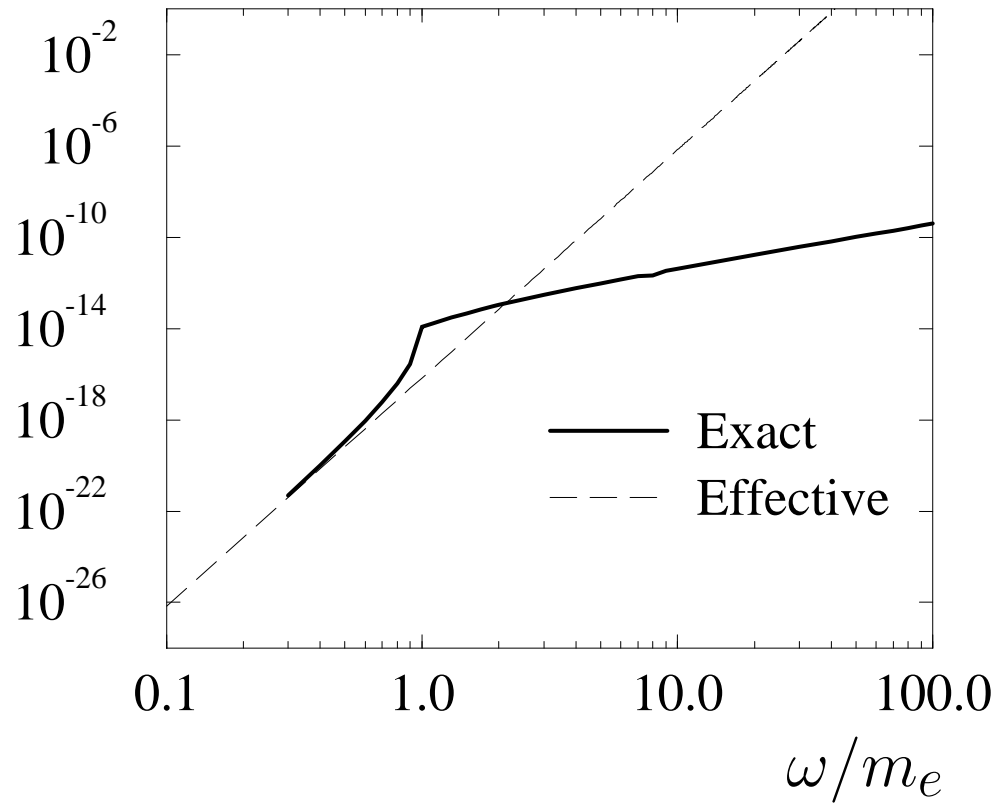


FIG. 4. $\nu\bar{\nu} \rightarrow \gamma\gamma\gamma$ cross section in fb as a function of ω/m_e .